UAV-based Measurement of Marine Vessels Smoke Plumes – Guidance and Control System

David Escudeiro
davidescudeiro@tecnico.ulisboa.pt
Instituto Superior Técnico, Universidade de Lisboa, Portugal
March 2018

***Abstract*—This work addresses the problem of designing a Guidance and Control (G&C) system for UAV-based monitoring of marine vessels gas emissions. A constant speed, fixed-wing UAV is considered for this purpose, aiming to track a slower vessel and provide enhanced conditions for the smoke plume gas measurements. The adopted solution can be separated into two parts: a path planning approach, in which a virtual reference point is generated, at each time instant, providing the desired trajectory for the UAV to satisfy the given mission restrictions; and a nonlinear control law design, to guarantee that the UAV heading rate converges to the reference trajectory. In terms of path planning, an oscillatory motion was adopted for the reference point, allowing for the compensation of the speed difference between both vehicles, while respecting the UAV maximum heading rate. For the control part, a novel error formulation is proposed, leading to a nonlinear design with global asymptotic stability guarantees, achieved by using Lyapunov-based methods for nonlinear cascade systems. The control law thus obtained is the main contribution of this work, as it solves the reference trajectory tracking control problem for a fixed-speed nonholonomic vehicle. Finally, the overall system is implemented and simulation results are presented to support the theoretical developments. Sufficient conditions to ensure the enforcement of the actuation bounds are introduced, and the performance of the novel error formulation is assessed.**

I. Introduction

Currently, more than 90% of world trade is being carried by marine vessels, as this is the most cost-effective way of moving en masse goods and raw materials all over the world [1]. According to a study done by the International Maritime Organization (IMO) [1], the annual average fuel consumption of all the ships in the world stands between 247 and 325 million tonnes of fuel, considering the time interval between 2007 and 2012.

Given the inevitable growth in the number of marine vessels operating in the oceans, due to its economic advantage over the other means of cargo transportation, the way to decelerate the trend of growth in emissions is to limit the impact of each individual ship in the global gas emissions. The MARPOL Convention developed in 1973 by the IMO was the first global effort to reduce the pollution of the ocean and seas, including dumping, oil, and air pollution.

More concretely the MARPOL Annex VI, first adopted in 1997 and extensively revised in 2008, imposes fixed limits on the main air pollutants contained in ship exhaust gases, including the sulphur and nitrous oxides, and other particulate matter. The most specific limit is presented in Regulation 14 of the MARPOL Annex VI [2], where different limits are applied for ships operating inside or outside a Sulphur Emission Control Area (SECA) – in the European Union (EU), the established SECAs cover the Baltic and the North Sea area, including the English Channel. While the limits on the SO_x shipping emissions outside a SECA are currently of 3.50% (m/m), inside this area these emissions are restricted to 0.1% [2], which requires an effective monitorization in order to ensure the rigorous limits are duly respected.

As the new limit for the shipping sulphur emissions in the SECAs entered into force in the beginning of 2015, some of the EU Member States around the SECA area joined forces to create the CompMon network. The CompMon project aims to provide a tighter control on compliance with the MARPOL Annex VI. This can be achieved through the use of remote sensing and sampling methods to measure the sulphur emissions of ships, in order to determine those who are possibly non-compliant. When some high sulphur concentration is found, the national enforcement authorities should receive this information, so they can proceed to more accurate on-board inspections [3].

With the evolution of technology leading to lighter and cheaper sniffer sensors, we believe the tendency for the future is to perform gas emission monitorization with UAVs, reducing both the risks and the costs, and increasing the efficiency of the measurements. Moreover, this monitorization will be needed also outside the SECA area, as the limits on the SO_x shipping emissions will decrease to 0.5% (m/m), requiring a significant increase in the monitoring means.

Being aware of the importance of monitoring the gas emissions of marine vessels, the main objective of this work is the development of a Guidance and Control System for an autonomous fixed-wing UAV, allowing for a robust tracking of a marine vessel, more precisely of its smoke plume.

The organization of this paper is as follows. In section II the considered mission goals and restrictions are described as well as the vehicles dynamics. Section III provides the description and analysis of the adopted guidance system. In Section IV a nonlinear controller is designed based on a proposed error formulation, commanding the UAV to converge to and track a feasible reference point. Section V presents some simulation-based results in order to support the theoretical developments. Finally, some concluding remarks are presented in Section VI.

II. Mission Description and Vehicle Dynamics

A. Mission Description

As this particular problem of the UAV-based monitorization of marine vessels gas emissions is still an emerging concern, there are few indications on the best way to guide the UAV to follow the smoke plume of the vessel and to perform the gas concentration measurements. The baseline for the definition of the mission conditions will be the best practices compilation reported in [4].

In the above-mentioned publication [4], different types of sensor systems available for the airborne measurement of vessels emissions and subsequent calculation of the FSC are presented. In the present work, the mini-sniffer sensor is considered, being a lightweight, low-cost sensor, capable of detecting the FSC with high precision. In order for the mini-sniffer sensor to operate properly, the UAV must get into physical contact with the smoke plume, collect a sample of the smoke through a gas inlet, and then the gas sensors will take some time to process and to estimate the concentrations of CO_2, SO_2 and NO_x. Moreover, several consecutive measurements should be performed, in order to provide a better estimate of the gas concentrations.

Therefore, the UAV should be able to fly through the smoke plume several consecutive times with a certain periodicity, preferable in a region close to the vessel, which is where the gas concentrations are higher. Additionally, for safety reasons, the UAV should maintain a minimum distance to the vessel, and thus, a keep-out area around the vessel is considered. The UAV should be able to remain outside of this region all the times.

B. Vehicle Dynamics

The relevant reference frames that will be used throughout this work are the inertial reference frame $\{I\}$, the UAV body-fixed frame $\{B\}$ and the vessel body-fixed frame $\{V\}$.

As the main purpose of this work is the design of a high-level guidance system, the considered fixed-wing UAV is modeled as a Dubins vehicle by

$$\dot{\mathbf{x}} = \begin{cases} \dot{x} = v\cos(\chi) \\ \dot{y} = v\sin(\chi) \\ \dot{\chi} = \omega \end{cases}, \tag{1}$$

where v and ω are the commanded speed and heading rate, respectively, that will be given to the inner-loop control, as well as the desired altitude h. The desired speed of the UAV will be denoted as V_r and is considered to be the optimal speed for a cruise flight condition. This dynamics is considered as a nonholonomic vehicle, as it satisfies the nonholonomic constraint $\dot{x}\sin\chi - \dot{y}\cos\chi = 0$.

An important restriction that should be taken in consideration during the guidance and control system design is the UAV maximum heading rate $\omega_{\max}$, that is the maximum absolute value of u that can be attained by the UAV.

The dynamics motion of the vessel can be defined with the same motion of the UAV, with speed $V_V \in [0, V_\mathrm{r}]$ instead of v, having a relatively low acceleration, and heading rate ω_V instead of ω, with ω_V significantly lower than ω. These assumptions of low linear acceleration and low heading rate for the vessel are reasonable, since the vessels considered in this mission are mostly very large, travelling in cruise speed for a long time, and having very low course deviations.

III. Guidance

This section provides the development of a guidance system which should be able to generate a reference trajectory for a fixed-wing UAV to follow a slower target – in this case a vessel. The generated trajectory should be: i) feasible by the UAV, ii) adjustable to different vessel speeds, and iii) outside and near the keep-out area around the vessel, passing through the smoke plume.

A. Problem statement

After some review on the existing target tracking techniques in the literature, one should choose the best solution that can be adapted to this study, in order to accomplish the proposed mission requirements. The considered target tracking problem is not trivial, as the fixed-wing UAV shall keep a constant speed for proper operation, while the target vessel is usually significantly slower.

The solution that seems to be more suitable is a path planning technique, where a virtual reference point is generated with the desired trajectory for the UAV, complying with the mission restrictions. This way a well-defined trajectory can be designed to cross the smoke plume in the desired point while respecting the minimum allowed distance to the vessel. Then a control law can be designed to command the UAV to converge to and track the reference point.

One should find a proper reference trajectory that can be valid for a wide range of possible vessel speeds, while respecting the dynamics of the UAV. Considering the work done in [5] and [6], the proposed oscillatory motion seems to have the potential to comply with the presented requirements, and mainly the ideas of [6] will be exploited in this work.

B. Proposed guidance solution

Firstly, the concept of Center of Oscillation (CO) is introduced. The CO is the virtual point to be placed in the smoke plume measurement site. This point is fixed in the vessel reference frame as long as the vessel keeps a constant velocity. The positioning of the CO will be addressed later in this chapter.

Secondly the reference point with position coordinates given by (x_r, y_r) is introduced. The reference point will be virtually generated with the desired motion of the , and can be seen as the desired point where the UAV should be at each time instant. The reference point motion is based on the oscillatory heading rate solution presented in [6], and can be modeled in the inertial reference frame as

$$\dot{\mathbf{x}}_r = \begin{cases} \dot{x}_\mathrm{r} = V_\mathrm{r}\cos(\chi_\mathrm{r}) \\ \dot{y}_\mathrm{r} = V_\mathrm{r}\sin(\chi_\mathrm{r}) \\ \dot{\chi}_\mathrm{r} = -A\sin\left(\omega_0 t + \phi_0\right) + \omega_V \end{cases} \tag{2}$$

where V_r is the desired UAV speed to be regulated by the autopilot and ω_V is the vessel heading rate. The initial position of the reference point will be coincident with the CO, and the former will have an oscillatory motion around the latter.

C. Analysis of the oscillation parameters

In order to better understand the behaviour of the reference point motion, the third equation in (2) is integrated to obtain an expression for the reference heading over time. For this analysis the vessel is considered to move with a constant velocity, having the constant speed V_V and the constant heading χ_V, leading to $\omega_V = 0$. Assuming that $\chi_\mathrm{r}(0) = A/\omega_0$,

$$\chi_\mathrm{r}(t) = \int_0^t \left[-A\sin\left(\omega_0\tau + \phi_0\right)\right] d\tau = \frac{A}{\omega_0}\cos\left(\omega_0 t + \phi_0\right). \tag{3}$$

For simplicity in this study, a new parameter is defined as $\eta = A/\omega_0$. Substituting (3) into the first and second equations of (2), one obtains

$$\begin{cases} \dot{x}_\mathrm{r}(t) = V_\mathrm{r}\cos\left[\eta\cos\left(\omega_0 t + \phi_0\right)\right] \\ \dot{y}_\mathrm{r}(t) = V_\mathrm{r}\sin\left[\eta\cos\left(\omega_0 t + \phi_0\right)\right] \end{cases}. \tag{4}$$

Given the periodic properties of both the $\sin$ and $\cos$ functions, one can see that, with this oscillatory heading solution, the reference point will advance in the X_I axis direction, while oscillating around the Y_I axis. Hence, considering a constant vessel speed, one can force the reference point to follow the vessel by adequately defining the average speed of the reference point over an oscillation period T. The mean speed of the reference point in a period T is given by

$$\begin{cases} \bar{\dot{x}}_\mathrm{r}(t) & = V_\mathrm{r}\frac{1}{T}\int_0^T \cos\left[\eta\cos\left(\omega_0 t\right)\right] dt = V_\mathrm{r}F(\eta) \\ \bar{\dot{y}}_\mathrm{r}(t) & = V_\mathrm{r}\frac{1}{T}\int_0^T \sin\left[\eta\cos\left(\omega_0 t\right)\right] dt = 0 \end{cases} \tag{5}$$

Let the ratio between vessel and reference speeds be given by $\nu = V_\mathrm{V}/V_\mathrm{r}$ and define the function $F(\eta) = \frac{1}{T}\int_0^T \cos\left[\eta\cos\left(\omega_0 t\right)\right] dt$. Then, having a mean speed of the reference point over a period equal to the vessel speed is equivalent to $V_\mathrm{V} = \bar{V}_\mathrm{r} \Leftrightarrow \nu = |F(\eta)|$. Hence, a relation between the speed ratio ν and parameter η is found. Therefore, this parameter η can be used to adjust the reference point mean speed in the X_I axis direction to the vessel speed, which requires the computation of the inverse of the Bessel function. The Bessel function is non-invertible in its full domain. However, in the problem at hand, it can be considered that the speed ratio is given by $\nu \in [0, 1]$, which covers the range from having a static vessel to having a vessel with the same speed as the UAV. The Bessel function $J_0(\eta)$ can then be inverted in a restrict domain between $\eta = 0$ and its first positive zero. The first positive zero of $J_0(\eta)$ can be found numerically, and is $\eta \approx 2.4048$.

Parameter η is then defined as a function of ν as

$$\eta(\nu) = J_0^{-1}(\nu). \tag{6}$$

It is highlighted that, in order to achieve the desired mean motion along the X_I axis, the initial heading of the reference point should be set according to

$$\chi_\mathrm{r}(t=0) = \Big[\eta\cos\left(\omega_0 t + \phi_0\right)\Big]_{t=0} = \eta\cos\phi_0. \tag{7}$$

Now that the reference point is able to follow the vessel motion through the tuning of variable η, another important constraint should be considered, that is the UAV maximum heading rate ω_max. Recalling the heading rate equation of the reference point (2) this restriction can be forced, and the oscillation frequency, ω_0, shall satisfy

$$\omega_0 \leq \frac{\omega_\mathrm{max} - \|\omega_V\|}{\eta(\nu)}. \tag{8}$$

The remaining parameter to be considered is the oscillation phase, ϕ_0. This parameter can be used to fix the initial position of the reference point in a different position of the periodic trajectory. This parameter will be used in the CO Positioning section.

D. Positioning of the Center of Oscillation (CO)

In the previous subsections, the generation of the reference point was described, based on an oscillatory motion around the CO. The goal of this subsection is to place the CO within the desired plume measurement site, so that the generated reference point trajectory complies with the proposed requirements. Ideally, the measurement site should be the closest possible to the vessel, but always respecting the keep-out area avoidance restriction.

The smoke plume direction is defined by means of its heading χ_P and elevation α_P, while the radius of the keep-out area around the vessel is represented by r_min. The position of the CO in the vessel reference frame is given by

$$\begin{cases} x_\mathrm{CO} = r_{CO}\cos\alpha_P\cos\chi_P \\ y_\mathrm{CO} = r_{CO}\cos\alpha_P\sin\chi_P \\ z_\mathrm{CO} = r_{CO}\sin\alpha_P \end{cases} \tag{9}$$

where r_{CO} is the three-dimensional distance between the vessel and the CO.

In order to ensure the reference trajectory never enters the keep-out area, one can relate r_{CO} with the maximum distance between the reference point and the CO, d_max, from

$$r_\mathrm{CO} = r_\mathrm{min} + d_\mathrm{max}(\chi_P)\cos\alpha_P, \tag{10}$$

where d_max depends on the wind direction and can be approximated by

$$\begin{aligned} d_\mathrm{max}(\nu, \chi_P) = {} & |d_\mathrm{x}(t,\nu)|_\mathrm{max} \\ & + \Big(|d_\mathrm{y}(t,\nu)|_\mathrm{max} - |d_\mathrm{x}(t,\nu)|_\mathrm{max}\Big)\,\|\sin\chi_P\|, \end{aligned} \tag{11}$$

with $|d_\mathrm{x}(t,\nu)|_\mathrm{max}$ and $|d_\mathrm{y}(t,\nu)|_\mathrm{max}$ being the maximum distance between the CO and the reference point in both horizontal coordinates. These maximum values of the distance in

the separated coordinates can be derived from the integration of both the vessel dynamics and (4), becoming

$$\begin{cases} |d_{\mathrm{x}}(t,\nu)|_{\max} = |d_{\mathrm{x}}\left(t_{\mathrm{x}}(\nu),\nu\right)| = V_{\mathrm{r}}\left|F_{\mathrm{x}}(t_{\mathrm{x}}(\nu),\nu) - \nu \cdot t_{\mathrm{x}}(\nu)\right| \\ |d_{\mathrm{y}}(t,\nu)|_{\max} = |d_{\mathrm{y}}\left(t_{\mathrm{y}},\nu\right)| = V_{\mathrm{r}}\left|F_{\mathrm{y}}(t_{\mathrm{y}},\nu)\right|, \end{cases} \tag{12}$$

defining the functions $F_{\mathrm{x}}(t,\nu) = \int \cos\left[\eta(\nu)\cos\left(\omega_0 t\right)\right] dt$ and $F_{\mathrm{y}}(t,\nu) = \int \sin\left[\eta(\nu)\cos\left(\omega_0 t\right)\right] dt$, and considering the time instants $t_{\mathrm{x}}(\nu) = \frac{1}{\omega_0}\arccos\left[\frac{1}{\eta}\arccos\left(\nu\right)\right]$ and $t_{\mathrm{y}} = \frac{\pi}{2\omega_0}$.

IV. Controller Design and Stability Proof

This section is devoted to the development of a control method for a fixed-wing UAV to track a virtual reference point, such as the one generated by the guidance system designed in the previous chapter. The results obtained in this chapter can be applied to a wide range of autonomous nonholonomic vehicles other than UAVs, such as underwater vehicles, underactuated vessels, cars, or other ground vehicles or robots with similar nonholonomic constraints. The main contribution of this thesis is presented in this section, which is a novel error formulation that eliminates the singularity presented on the line-of-sight tracking of a constant-speed vehicle.

A. Control problem statement

The main target tracking problem of this work is first addressed in the previous section. The first key challenge was due to the speed differential between the target and the pursuer vehicle. With the generation of a virtual reference point moving with the desired trajectory for the pursuer, the challenge becomes to track a target with the same speed and a feasible motion. It is important to note that all the dynamics considered in this chapter are written in the two-dimensional horizontal plane, considering a top-view of the environment.

Consider all types of nonholonomic vehicles that can be represented as a unicyle – or the so-called Dubins vehicle – by the equations of motion in (1). The main limitation of this dynamics is due to the absence of lateral velocity and is characterized by the nonholonomic constraint $\dot{y}\cos\chi - \dot{x}\sin\chi = 0$. Moreover, consider that a feasible reference trajectory is given and that it can be represented by

$$\dot{\mathbf{x}}_{\mathrm{r}} = \begin{cases} \dot{x}_{\mathrm{r}} = v_{\mathrm{r}}\cos(\chi_{\mathrm{r}}) \\ \dot{y}_{\mathrm{r}} = v_{\mathrm{r}}\sin(\chi_{\mathrm{r}}) \\ \dot{\chi}_{\mathrm{r}} = \omega_{\mathrm{r}} \end{cases}. \tag{13}$$

The feasible reference speed v_{r} and heading rate ω_{r} functions should be suitable for the considered pursuer. In the particular case of a UAV, as considered in this work, the reference speed should be a constant value, ideally the optimal speed for a cruise flight condition. In order to extend the applications of the following results in this section, the reference heading rate will be considered to be a generic bounded and smooth function, that can be either a constant or a time varying function. Moreover, in order to comply with subsequent requirements, the derivative of the reference heading rate should be also bounded, i.e., $\dot{\omega}_{\mathrm{r}} \leq (\dot{\omega}_{\mathrm{r}})_{\max}$.

Defining the horizontal coordinates of the pursuer vehicle and the reference point in the inertial reference frame $\{I\}$ as $\mathbf{p} = (x,y)^T$ and $\mathbf{p}_{\mathrm{r}} = (x_{\mathrm{r}},y_{\mathrm{r}})^T$, respectively, the geometry of the tracking control problem is illustrated in Figure 1:

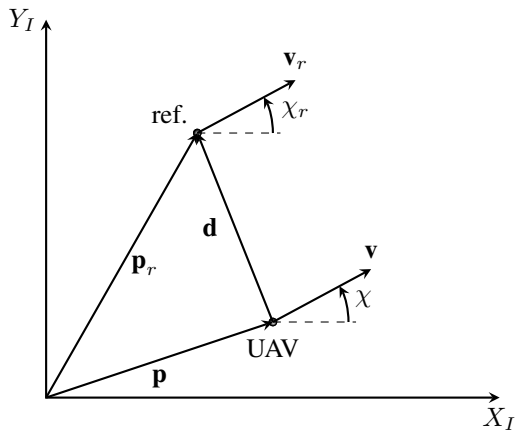

Figure 1: Geometry of the tracking control problem.

The velocity of the chaser can then be represented by $\dot{\mathbf{p}} = \mathbf{v} = \mathcal{R}(\chi)\begin{bmatrix} V_{\mathrm{r}} & 0 \end{bmatrix}^T$, and the analogous stands for the reference velocity $\dot{\mathbf{p}}_{\mathrm{r}} = \mathbf{v}_{\mathrm{r}}$. The standard rotation matrix $\mathcal{R}(\alpha)$ is defined as the two-dimensional right-handed rotation by an angle α, and its time derivative is denoted as $\dot{\mathcal{R}}(\alpha) = \mathcal{R}(\alpha)\mathcal{S}\left(\dot{\alpha}\right)$ In the present section, the commanded pursuer speed will be considered to match that of the reference, i.e. $v = V_{\mathrm{r}}$.

The main objective of the tracking control problem is to control the pursuer position to the reference position, $\mathbf{p} \to \mathbf{p}_{\mathrm{r}}$, as well as the pursuer velocity to the reference velocity vector, $\mathbf{v} \to \mathbf{v}_{\mathrm{r}}$. The latter control objective for the velocity vector can be posed only as a heading direction objective, $\chi \to \chi_{\mathrm{r}}$, since the speed V_{r} is considered to be controlled separately by an inner-loop controller. Since the relative positions can be represented by the distance vector as $\mathbf{d} = \mathbf{p}_{\mathrm{r}} - \mathbf{p}$, the former objective can be stated as $\mathbf{d} \to 0$. Therefore, the analysis taken in this section will aim to reach this control objective asymptotically, satisfying all the aforementioned contraints.

Despite the vast research carried out in the last decades on the guidance and control of autonomous vehicles, the tracking control problem addressed in this work is still an open topic for highly-constrained vehicles such as fixed-wing UAVs. The existing solutions in terms of the tracking control of unicycle-like vehicles consider two degrees-of-freedom for actuation, both the speed and the heading rate. However, the control challenge that emerged in the current study is confined to just one degree-of-freedom, since the only control input is the UAV heading rate – the speed and altitude are taken as constants.

A vast literature on the topic of nonholonomic tracking control can be found, for instance, in [7, 8, 9, 10, 11, 12, 13, 14]. However, from the existing solutions on the nonholonomic tracking control, there is no suitable result for the needs of the tracking control problem at hand.

An alternative approach to guide a UAV to track a reference point is proposed in the previously cited paper [6]. The same oscillatory motion is considered for the generation of a virtual reference point and a guidance law is suggested for the UAV to track the reference. This guidance law is based on the line-of-sight between the UAV and the reference point, but this is not defined when the UAV coincides with the reference point, representing a singularity of the algorithm, which is to be avoided in control laws. Moreover, the relative angle rate can reach very high values for certain initial conditions, leading to unfeasible heading rate commands. This is a great challenge on the tracking control problem when only the heading rate control is available, and will be analysed in more detail in the following section, where a novel error formulation is derived, leading to global stability of the tracking problem at hand.

B. Derivation of the error formulation

Consider the geometry of the control problem illustrated in Figure 1. Additionally, consider a new vector $\boldsymbol{\delta}$ with norm denoted by δ, with its origin in the reference point, and having the same heading as that of the reference velocity, χ_r. Hence, the new vector can be represented by $\boldsymbol{\delta} = \mathcal{R}(\chi_\mathrm{r}) \begin{bmatrix} \delta & 0 \end{bmatrix}^T$. Now consider the direct line-of-sight vector as $\mathbf{d} = \mathbf{p}_r - \mathbf{p} = \mathcal{R}(\chi_d) \begin{bmatrix} d & 0 \end{bmatrix}^T$, and define its norm as $d = \|\mathbf{d}\|$. Additionally, define a new relative vector $\mathbf{z}$, with norm $\rho = \|\mathbf{z}\|$, being the sum of the direct line-of-sight $\mathbf{d}$ with the new virtual vector $\boldsymbol{\delta}$, i.e.,

$$\mathbf{z} = \mathbf{p}_\mathrm{r} - \mathbf{p} + \boldsymbol{\delta} = \mathbf{d} + \boldsymbol{\delta}, \qquad \|\boldsymbol{\delta}\| = \delta > 0. \tag{14}$$

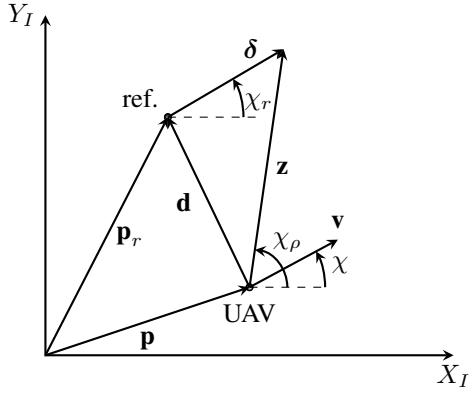

Figure 2: Geometry of the proposed tracking control approach, with new variable δ

This formulation of the tracking control problem is depicted in Figure 2. The heading of the relative vector $\mathbf{z}$, here defined as χ_ρ, will be the desired heading for the proposed control methodology. This new approach allows avoiding the singularity when the UAV position coincides with that of the reference point. It can be noticed that, with the UAV on top of the reference point, the relative heading χ_ρ becomes exactly the reference heading χ_r.

Now it is still left to find a proper expression for variable δ so that the singularity becomes unreachable. Having a value of δ always greater than the distance d it is possible to ensure that the singularity is never reached, as the vector $\mathbf{z}$ is always well-defined. Hence, the approach proposed in this work is to have an adaptive δ, able to change its value according to the current distance, d, between the UAV and the reference point. The adaptive δ is defined as

$$\delta\left(d^2\right) = \varepsilon d^2 + R, \tag{15}$$

where ε and R are positive constants to be tuned later. In order to ensure that ρ has a proper lower-bound, with δ being always larger that d, the control parameters should respect the relation $R > 1/(4\varepsilon)$.

Here the new error state dynamics will be derived, which will be considered as the nominal system for the purpose of this work. Consider the relative vector $\mathbf{z}$, defined in (14). This relative vector can also be written in inertial coordinates as $\mathbf{z} = \mathcal{R}(\chi_\rho) \begin{bmatrix} \rho & 0 \end{bmatrix}^T$, and thus, both representations of vector $\mathbf{z}$ can be equated,

$$\mathcal{R}(\chi_\rho) \begin{bmatrix} \rho & 0 \end{bmatrix}^T = \mathbf{p}_\mathrm{r} - \mathbf{p} + \boldsymbol{\delta}. \tag{16}$$

Now differentiating both sides of the previous equation with respect to time, and assuming the heading rate of the relative vector to be $\omega_\rho = \dot{\chi}_\rho$, it follows

$$\begin{aligned} &\mathcal{S}(\omega_\rho)\mathcal{R}(\chi_\rho) \begin{bmatrix} \rho & 0 \end{bmatrix}^T + \mathcal{R}(\chi_\rho) \begin{bmatrix} \dot{\rho} & 0 \end{bmatrix}^T \\ &\quad = V_\mathrm{r}\left[\mathcal{R}(\chi_\mathrm{r}) - \mathcal{R}(\chi)\right] + \delta\mathcal{S}(\omega_r)\mathcal{R}(\chi_r) + \dot{\delta}\mathcal{R}(\chi_r). \end{aligned} \tag{17}$$

Consider a local reference frame $\{Z\}$, centered and fixed in the UAV position, with its X_Z axis aligned with the direction of vector $\mathbf{z}$. In order to represent (17) in reference frame $\{Z\}$, a rotation by an angle χ_ρ is applied. Define also the relative angles $\phi_\mathrm{r} = \chi_\mathrm{r} - \chi_\rho$ and $\phi = \chi - \chi_\rho$. Applying some basic linear algebra to the previous equation, one gets the expressions to properly define the relative vector dynamics, respectively the linear $\dot{\rho}$ and angular ω_ρ velocities,

$$\begin{bmatrix} \dot{\rho} \\ \rho\omega_\rho \end{bmatrix} = \begin{bmatrix} V_\mathrm{r}\cos\phi_\mathrm{r} - V_\mathrm{r}\cos\phi - \delta\omega_\mathrm{r}\sin\phi_\mathrm{r} + \dot{\delta}\cos\phi_\mathrm{r} \\ V_\mathrm{r}\sin\phi_\mathrm{r} - V_\mathrm{r}\sin\phi + \delta\omega_\mathrm{r}\cos\phi_\mathrm{r} + \dot{\delta}\sin\phi_\mathrm{r} \end{bmatrix} \tag{18}$$

With the proposed relative formulation, it can be concluded that at least four state variables are required. The triangle formed by vectors $\mathbf{z}$, $\mathbf{d}$ and $\boldsymbol{\delta}$, needs three variables to be completely defined, without ambiguities. For the definition of this triangle it will be considered the norm of the relative vector, ρ, and variables ϕ_r and δ representing vector $\boldsymbol{\delta}$. The norm of the remaining vector, d, can be written from the stated variables δ, ρ and ϕ_r, as it will be derived next. Additionally, variable ϕ should also be included in order to specify the direction of the UAV velocity.

Therefore, the considered state variables, fully describing the dynamics of interest of the system are

$$\mathbf{x} = \begin{bmatrix} \delta & \rho & \phi_r & \phi \end{bmatrix}^T \tag{19}$$

Now the time-derivatives of the state are defined in terms of the state variables, so that the system dynamics can be completely characterized without any exogenous terms. It is only left to find an expression for the derivative $\dot{\delta}$. Firstly, the norm of the difference vector between the UAV and the reference point is related with the state variables. By definition, the distance, d, can be written as $d = \sqrt{\left[\left(x_\mathrm{r} - x\right)^Z\right]^2 + \left[\left(y_\mathrm{r} - y\right)^Z\right]^2}$.

From the problem geometry it follows that $\left(x_\mathrm{r} - x\right)^Z = \rho - \delta\cos\phi_\mathrm{r}$ and $\left(y_\mathrm{r} - y\right)^Z = -\delta\sin\phi_\mathrm{r}$. The squared norm of the distance vector is then given by $d^2 = \rho^2 + \delta^2 - 2\rho\delta\cos\phi_\mathrm{r}$. Now computing the time derivative of the previous equation and considering the result of equations (18), as well as the time derivative $\dot{\phi}_\mathrm{r} = \omega_\mathrm{r} - \omega_\rho$, we get

$$\frac{d}{dt}d^2 = -2V_\mathrm{r}\Big[\rho\big(\cos\phi - \cos\phi_\mathrm{r}\big) + \delta\Big(1 - \cos\big(\phi_\mathrm{r} - \phi\big)\Big)\Big] \tag{20}$$

Now from the previous result and from the definition of δ in (15), one can find its time derivative, $\dot{\delta}$. Hence, the nominal system dynamics is given by

$$\dot{\mathbf{x}} = \begin{cases} \dot{\delta} & = -2\varepsilon V_\mathrm{r}\Big[\rho\big(\mathrm{c}\phi - \mathrm{c}\phi_\mathrm{r}\big) + \delta\big(1 - \mathrm{c}\phi\phi_\mathrm{r}\big)\Big] \\ \dot{\rho} & = V_\mathrm{r}\big(\mathrm{c}\phi_\mathrm{r} - \mathrm{c}\phi\big) - \delta\omega_\mathrm{r}\mathrm{s}\phi_\mathrm{r} \\ & \quad -2\varepsilon V_\mathrm{r}\mathrm{c}\phi_\mathrm{r}\Big[\rho\big(\mathrm{c}\phi - \mathrm{c}\phi_\mathrm{r}\big) + \delta\big(1 - \mathrm{c}\phi\phi_\mathrm{r}\big)\Big] \\ \dot{\phi}_\mathrm{r} & = \omega_\mathrm{r} - \frac{1}{\rho}\big(V_\mathrm{r}\mathrm{s}\phi_\mathrm{r} - V_\mathrm{r}\mathrm{s}\phi + \delta\omega_\mathrm{r}\mathrm{c}\phi_\mathrm{r}\big) \\ & \quad +2\varepsilon V_\mathrm{r}\mathrm{s}\phi_\mathrm{r}\Big[\mathrm{c}\phi - \mathrm{c}\phi_\mathrm{r} + \frac{\delta}{\rho}\big(1 - \mathrm{c}\phi\phi_\mathrm{r}\big)\Big] \\ \dot{\phi} & = \omega - \frac{1}{\rho}\big(V_\mathrm{r}\mathrm{s}\phi_\mathrm{r} - V_\mathrm{r}\mathrm{s}\phi + \delta\omega_\mathrm{r}\mathrm{c}\phi_\mathrm{r}\big) \\ & \quad +2\varepsilon V_\mathrm{r}\mathrm{s}\phi_\mathrm{r}\Big[\mathrm{c}\phi - \mathrm{c}\phi_\mathrm{r} + \frac{\delta}{\rho}\big(1 - \mathrm{c}\phi\phi_\mathrm{r}\big)\Big] \end{cases} \tag{21}$$

where $\mathrm{c}\phi \triangleq \cos\phi$, $\mathrm{c}\phi_\mathrm{r} \triangleq \cos\phi_\mathrm{r}$, $\mathrm{s}\phi \triangleq \sin\phi$, $\mathrm{s}\phi_\mathrm{r} \triangleq \sin\phi_\mathrm{r}$ and $\mathrm{c}\phi\phi_\mathrm{r} \triangleq \cos\big(\phi - \phi_\mathrm{r}\big)$.

C. Lyapunov-based controller

The control objective defined earlier in this section is to follow the trajectory of a reference point, which is considered to have a feasible motion for the pursuer vehicle. Hence, the tracking objective is depicted by ensuring that both $\mathbf{d} \to 0$ and $\chi \to \chi_\mathrm{r}$. The derived relative dynamics will be considered for the controller derivation, with the control objective being now defined as $\mathbf{x} \to \mathbf{x}_d$, where $\mathbf{x}$ is given by (19) and $\mathbf{x}_d = \begin{bmatrix} R & R & 0 & 0 \end{bmatrix}^T$.

Here a steering control law will be derived, acting only on the UAV heading rate, ω, being able to lead the four-state model to the desired equilibrium point, and thus leading the UAV to the reference trajectory. Stability will be proved through the use of the Lyapunov theory. Firstly, looking upon the control objective of leading the distance, d, to zero, and regarding only the state variables associated with the positional relations of the system, here defined as $\mathbf{x}_1 = (\delta, \rho, \phi_\mathrm{r})$ and which are not directly controllable, consider the Lyapunov function candidate

$$V_1\left(\mathbf{x}_1\right) = \frac{1}{2}d^2\left(\mathbf{x}_1\right) = \frac{1}{2}\left(\rho^2 + \delta^2 - 2\rho\delta\cos\phi_\mathrm{r}\right). \tag{22}$$

In order to guarantee stability, a Lyapunov function must be positive definite and its derivative must be at least negative semi-definite (Theorem 4.1 in [15]). Checking the requirement of positive-definiteness for V_1,

- $V_1\left(\mathbf{x}_1 = \mathbf{x}_{1_d}\right) = 0$,
- $V_1\left(\mathbf{x}_1\right) > 0 \;\; \forall\, \mathbf{x}_1 \neq 0$.

Hence $V_1\left(\mathbf{x}_1\right)$ is a positive definite function, and its derivative should be evaluated. From the result of (20) the derivative of $V_1\left(\mathbf{x}_1\right)$ becomes

$$\begin{aligned} \dot{V}_1\left(\mathbf{x}_1\right) = &-\rho V_\mathrm{r}\big(1 - \cos\phi_\mathrm{r}\big) - \delta V_\mathrm{r}\Big(1 - \cos\big(\phi_\mathrm{r} - \phi\big)\Big) \\ &+ \rho V_\mathrm{r}\big(1 - \cos\phi\big). \end{aligned} \tag{23}$$

The derivative $\dot{V}_1$ is not necessarily negative and thus the function V_1 can not be considered a Lyapunov function, which was already expected since it considers the uncontrolled system. Consider the control law

$$\omega = -\,k_1\rho V_\mathrm{r}\frac{\sin\phi}{1 + \cos\phi} + \omega_\rho, \tag{24}$$

where ω_ρ is defined in (18). Now a composite Lyapunov function candidate for the whole system (21) with controller (24) can be defined as

$$V_2\left(\mathbf{x}\right) = V_1\left(\mathbf{x}_1\right) + k_2\big(1 - \cos\phi\big). \tag{25}$$

This new function also satisfies the positive-definiteness requirements. Considering the controlled system, and choosing k_2 such that $k_1 k_2 = 1$ we get a negative semidefinite derivative,

$$\dot{V}_2\left(\mathbf{x}\right) = -\rho V_\mathrm{r}\big(1 - \cos\phi_\mathrm{r}\big) - \delta V_\mathrm{r}\Big(1 - \cos\big(\phi_\mathrm{r} - \phi\big)\Big) \leq 0. \tag{26}$$

Hence, the requirements for considering $V_2\left(\mathbf{x}\right)$ a Lyapunov function are fulfilled and stability of system (21) is guaranteed with controller (24). However, the weaker condition of negative semidefiniteness of the Lyapunov function derivative alone is not enough to prove asymptotic stability of the system, and further analysis should be made.

Consider a time-varying, bounded reference heading rate $\omega_\mathrm{r}(t)$, with a bounded time-derivative $\dot{\omega}_\mathrm{r}(t)$. In order to assess the asymptotic stability of the non-autonomous system, consider again the Lyapunov function $V_2\big(\mathbf{x}\big)$ (25) with time-derivative $\dot{V}_2\big(\mathbf{x}\big)$ (26).

The *Lyapunov-Like Lemma* stated in [16] (Lemma 4.3) can be applied here. It states that if the Lyapunov function $V_2(\mathbf{x})$ satisfies the conditions

- $V_2(\mathbf{x})$ is lower bounded,
- $\dot{V}_2(\mathbf{x})$ is negative semi-definite,
- $\dot{V}_2(\mathbf{x})$ is uniformly continuous in time,

then $\dot{V}_2(\mathbf{x}) \to 0$ as $t \to \infty$.

The first two conditions are verified from the definition of Lyapunov function. The negative semidefiniteness of the derivative $\dot{V}_2(\mathbf{x})$ implies that $V_2(t) \leq V_2(t_0), \quad \forall t > t_0$, and hence, that ρ, ϕ_r, ϕ and δ are bounded.

To check whether $\dot{V}_2$ is uniformly continuous, its time derivative should be found,

$$\ddot{V}_2 = -V_\mathrm{r}\Big[\dot{\rho}\big(1-\cos\phi_\mathrm{r}\big) + \rho\dot{\phi}_r \sin\phi_\mathrm{r} + \big(\dot{\phi}_r - \dot{\phi}\big)\delta\sin\big(\phi_\mathrm{r}-\phi\big) + \dot{\delta}\Big(1-\cos\big(\phi_\mathrm{r}-\phi\big)\Big)\Big]. \tag{27}$$

Since $\omega_\mathrm{r}(t)$ is bounded by hypothesis, and the state variables were shown to be bounded, then the state derivatives $\dot{\delta}$, $\dot{\rho}$, $\dot{\phi}_\mathrm{r}$ and $\dot{\phi}$ are also bounded. Hence, $\ddot{V}_2$ is bounded, implying that $\dot{V}_2$ is uniformly continuous in time.

With all the conditions satisfied, the *Lyapunov-Like Lemma* [16] can be applied, proving that $t \to \infty \Rightarrow \dot{V}_2(\mathbf{x}, t) \to 0$. From the expression for the Lyapunov function derivative (26) it follows that

$$\dot{V}_2(\mathbf{x}, t) \to 0 \Rightarrow \phi_\mathrm{r}(t), \phi(t) \to 0. \tag{28}$$

Now, given the time-dependency of the system, the implication $\phi_\mathrm{r}(t) \to 0 \Rightarrow \dot{\phi}_\mathrm{r}(t) \to 0$ cannot be readly assumed. However, it can be confirmed applying *Barbalat's Lemma* [16] to function $\dot{\phi}_\mathrm{r}$, defined in (21), since the state variables and derivatives are bounded, as shown above, and given the boundedness of the reference heading rate derivative, $\dot{\omega}_\mathrm{r}(t)$, which all lead to the uniform continuity of $\ddot{\phi}_\mathrm{r}(t)$. Note that it is here assumed the boundedness of the term $1/\rho$, which is achieved by a proper tuning of variables ε and R, as stated previously. Hence, it is proved that, if ϕ_r converges to zero as $t \to \infty$, then $\dot{\phi}_\mathrm{r}$ also converges to zero, i.e.,

$$\phi_\mathrm{r}(t) \to 0 \Rightarrow \dot{\phi}_\mathrm{r}(t) \to 0. \tag{29}$$

Therefore, given $\phi_\mathrm{r}(t), \phi(t), \dot{\phi}_\mathrm{r}(t) \to 0$ as $t \to \infty$, from the expression of $\dot{\phi}_\mathrm{r}(t)$ (21) we get $\rho(t) \to \delta(t)$, as long as $\omega_\mathrm{r}(t) \neq 0$. By definition in the problem formulation, $\rho(t) \to \delta(t)$ implies that $d(t) \to 0$ and thus $\delta(t) \to R$. Hence, it is proved that $\mathbf{x}_0 \in D \Rightarrow \mathbf{x}(t) \to \mathbf{x}_d$ as $t \to \infty$, and then, the non-autonomous system (21) in closed-loop with (24) is asymptotically stable.

D. Nonlinear cascade system approach

Despite the Lyapunov method being able to give sufficient conditions to prove stability of nonlinear systems, the definition of a Lyapunov function for the full system is not a necessary condition to prove global stability. In this section, in order to generalize the problem at hand, a different approach will be used to achieve global asymptotic stability of system (21), with a class of controllers described by

$$\omega\big(t, \mathbf{x}\big) = -h(\phi) + \omega_\rho\big(t, \mathbf{x}\big), \tag{30}$$

where $h(\phi)$ must satisfy $h(0) = 0$ and $\phi h(\phi) > 0$, $\forall \phi \in [-\pi, \pi]$. Consider the closed-loop system (21) with a controller of the type (30), represented as a nonlinear non-autonomous cascaded system of the form

$$\dot{\mathbf{x}}_1 = f_1(t, \mathbf{x}_1, \mathbf{x}_2), \tag{31a}$$

$$\dot{\mathbf{x}}_2 = f_2(\mathbf{x}_2), \tag{31b}$$

where $\mathbf{x}_1 = \begin{bmatrix}\delta & \rho & \phi_\mathrm{r}\end{bmatrix}^T$ and $\mathbf{x}_2 = \phi$.

As described in [15], Lemma 4.7, the global stability of this kind of cascade systems can be assessed if either subsystem (31a) is input-to-state stable, having $\mathbf{x}_2$ as input, and if subsytem (31b) is globally asymptotically stable.

Thus, in order to assess the requirements for the previous system to be input-to-state stable, one should first evaluate the stability of the unforced system

$$\dot{\mathbf{x}}_1 = f_1(t, \mathbf{x}_1, 0) = \begin{cases} \dot{\delta} & = -2\varepsilon\big(\rho+\delta\big)\big(1-\mathrm{c}\phi_\mathrm{r}\big) \\ \dot{\rho} & = -V_\mathrm{r}\big(1-\mathrm{c}\phi_\mathrm{r}\big) - \delta\omega_\mathrm{r}(t)\mathrm{s}\phi_\mathrm{r} \\ & \quad -2\varepsilon V_\mathrm{r}\mathrm{c}\phi_\mathrm{r}\big(\rho+\delta\big)\big(1-\mathrm{c}\phi_\mathrm{r}\big) \\ \dot{\phi}_\mathrm{r} & = \omega_\mathrm{r}(t) - \frac{1}{\rho}\Big[V_\mathrm{r}\mathrm{s}\phi_\mathrm{r} + \delta\omega_\mathrm{r}(t)\mathrm{c}\phi_\mathrm{r} \\ & \quad -2\varepsilon V_\mathrm{r}\mathrm{s}\phi_\mathrm{r}\big(\rho+\delta\big)\big(1-\mathrm{c}\phi_\mathrm{r}\big)\Big] \end{cases}. \tag{32}$$

Now recall the Lyapunov function candidate V_1, introduced in previous section (22). Evaluating its derivative over the unforced system (32) we get

$$\dot{V}_1\left(\mathbf{x}_1\right) = -V_\mathrm{r}\big(\rho+\delta\big)\big(1-\cos\phi_\mathrm{r}\big) \leq 0. \tag{33}$$

The resulting derivative $\dot{V}_1$ is negative semidefinite, and thus, function V_1 is a Lyapunov function for the unforced system (32). However, the input-to-state stability condition requires a negative derivative of the Lyapunov function, as stated in Theorem 4.19 in [15], and thus it cannot be applied to the considered system.

In literature, there are several authors presenting some sufficient conditions to prove global asymptotic stability of cascade systems where only a negative semidefinite Lyapunov function derivative is achievable. While some authors consider the global stability of nonlinear autonomous cascade systems, [17, 18, 19], others go even further and present sufficient conditions for nonlinear time-varying cascade systems [20, 21, 22]. Accordingly, the global asymptotic stability of the controlled system around the equilibrium $\mathbf{x}_d$ is achieved if both

systems (31b) and (32) are globally asymptotically stable and also if all the trajectories of the system are bounded.

The first condition for the global asymptotic stability of the origin of (31b) is straightforward since $\dot{\mathbf{x}}_2 = f(\mathbf{x}_2) = -h(\phi)$, and given the stated conditions for function $h(\phi)$.

Consider again the Lyapunov function V_1, which has the time derivative (33), evaluated over the unforced system (32). Since $\dot{V}_1(\mathbf{x}_1) \leq 0$, then $V_1(t) \leq V_1(t_0)$ and hence $\mathbf{x}_1$ is bounded. To check whether $\dot{V}_1$ is uniformly continuous, its derivative should be found,

$$\ddot{V}_1(\mathbf{x}_1) = -V_\mathrm{r}\big(\dot{\rho}+\dot{\delta}\big)\big(1-\cos\phi_\mathrm{r}\big) - V_\mathrm{r}\big(\rho+\delta\big)\dot{\phi}_\mathrm{r}\sin\phi_\mathrm{r}. \quad (34)$$

Since $\omega_\mathrm{r}(t)$ is bounded by hypothesis, and the state variables $\mathbf{x}_1$ were shouwn to be bounded, then the state derivatives $\dot{\delta}$, $\dot{\rho}$ and $\dot{\phi}_r$ are also bounded. Hence, $\ddot{V}_1$ is bounded, proving that $\dot{V}_1$ is uniformly continuos, and thus, from the *Lyapunov Like-Lemma* [16], we prove that $\dot{V}_1(t,\mathbf{x}_1) \to 0$ as $t \to \infty$.

From the previous expression for $\dot{V}_1$, it follows that $\dot{V}_1(t,\mathbf{x}_1) \to 0 \Rightarrow \phi_\mathrm{r}(t) \to 0$. Using the *Barbalat's Lemma* [16] as in the previous section, we prove also that $\phi_\mathrm{r}(t) \to 0 \Rightarrow \dot{\phi}_\mathrm{r}(t) \to 0$. Therefore, from the third equation in (32) it is proved that $\dot{\phi}_\mathrm{r}(t) \to 0 \Rightarrow \rho(t) \to \delta(t)$. Hence, it is proved that $\mathbf{x}_1(t) \to \mathbf{x}_{1_d}$ as $t \to \infty$, and thus, the equilibrium $\mathbf{x}_{1_d}$ is a globally asymptotically stable equilibrium of the unforced system (32).

Now it is only left to prove that all the trajectories of the full system (31) are bounded. This condition comes from the fact that subsystem (31a) does not explode when ϕ is not zero. In the worst situation, the distance can be always increasing while ϕ is converging to zero (through the dynamics of $\dot{\mathbf{x}}_2$), and if variable ϕ converges to zero very slowly, the distance d can increase significantly. However, from the result in (23), the derivative of Lyapunov function V_1 can be written in the form

$$\dot{V}_1(t,\mathbf{x}_1) = -\rho V_\mathrm{r}\big(\cos\phi - \cos\phi_\mathrm{r}\big) - \delta V_\mathrm{r}\Big(1-\cos\big(\phi-\phi_\mathrm{r}\big)\Big). \quad (35)$$

Thus, proceeding with the previous reasoning, when variable ϕ is converging to zero, there is a time instante after which $\phi \leq \phi_r$, and thus $\cos\phi \geq \cos\phi_\mathrm{r}$. From this time instant on, the distance no longer increases and, hence, all the trajectories of the system (31) are bounded.

Hence, with the three conditions being verified, it is proved that $\mathbf{x}_d$ is a globally asymptotically stable equilibrium for the system in (31).

V. Simulations and Results

After the development of the separated Guidance and Control sub-systems, described in the previous sections, the overall system is now implemented and the more relevant results are presented in this section. Firstly, a simulation is presented in Figure 3 where the controller derived in the previous section – with the proposed error formulation – is used for a UAV to follow a circular reference trajectory.

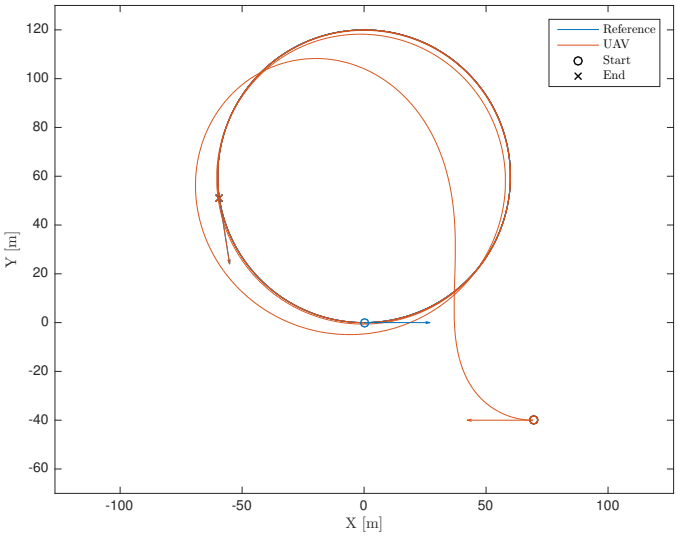

Figure 3: Sim. 1 – UAV tracking a reference point with circular trajectory, using the proposed control law.

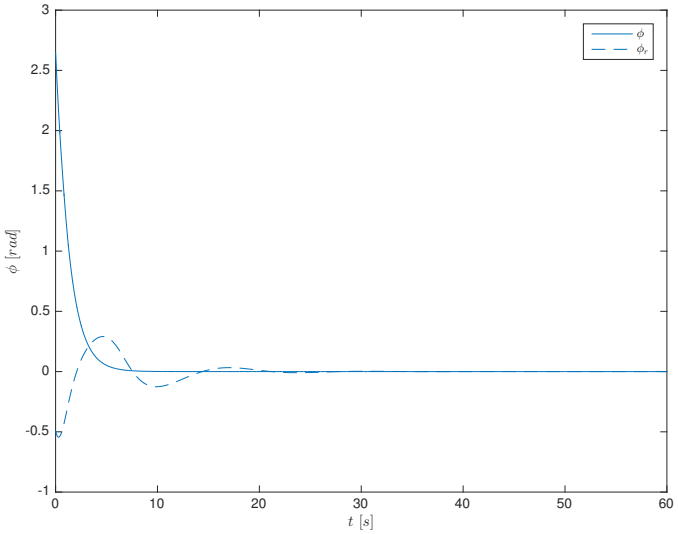

Figure 4: Sim. 1 – Representation of the state variables ϕ and ϕ_r over time.

The initial headings of both the UAV and the reference are in opposite directions and thus $\phi(0) \neq 0$, as depicted in Figure 4. In this figure, the asymptotical stability of system (31b) is evident, as considered in the previous section. It is also possible to notice that when $\phi < \phi_\mathrm{r}$ and thus $\cos\phi > \cos\phi_\mathrm{r}$, the system behaves as the unforced system (32). Looking also to Figure 5 it can be confirmed that once the system behaves as (32) then the distance no longer increases. Additionally, there are some saddle points depicted in Figure 5, corresponding to the time instants when $\phi_\mathrm{r} = \phi$, and thus to having $\dot{V}_1 = 0$, confirming the negative semidefinite condition of the derivative (26). With this simulation, the results of the previous section are confirmed, especially the asymptotic stability of the controlled system – the global condition cannot be confirmed

with only one simulation, however, intuitively it seems to be valid.

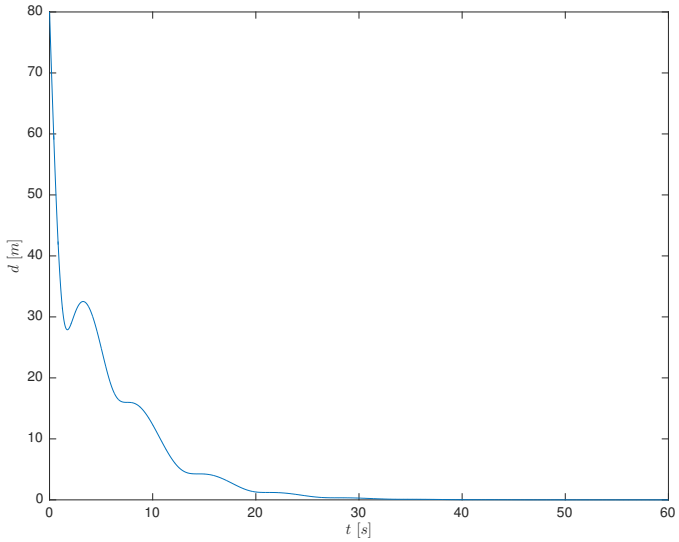

Figure 5: Sim. 1 – Representation of the distance d between the UAV and the reference point over time.

A second simulation is now performed, in order to compare the controller using the proposed formulation, with a simple proportional controller based on the line-of-sight between the UAV and the reference point. In Figure 6 the trajectories of two UAVs are depicted, with UAV 1 using the line-of-sight based controller and UAV 2 using the controller derived from the proposed δ-formulation. An extreme scenario is posed in this simulation, with the UAVs starting in front of the reference point and moving in the opposite direction.

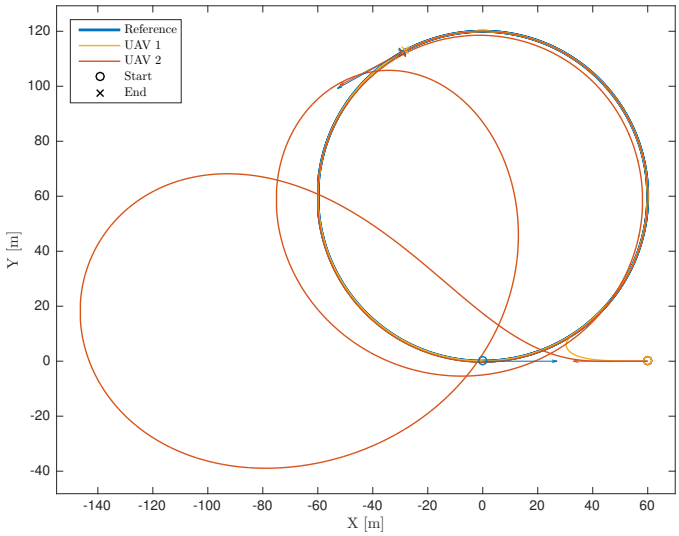

Figure 6: Sim. 2 – Comparison between the proposed control method and the line-of-sight control approach.

Despite the fast convergence of UAV 1 to the reference point, the actuators would saturate as the system approach the singularity, as can be observed in Figure 7. UAV 2, in turn, is able to converge to and track the reference point with a feasible heading rate, which is possible due to the adjustment of the control parameters ε and R from the proposed formulation. This is a significant advantage of the proposed formulation, as it is able to completely eliminate the singularity present in this tracking control problem.

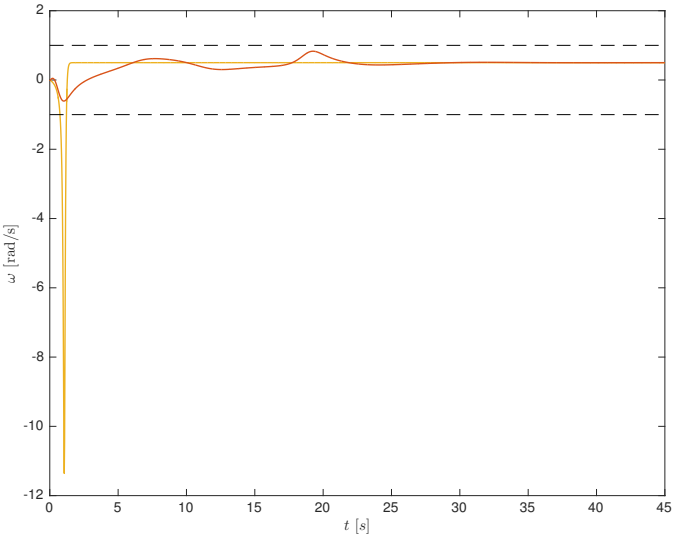

Figure 7: Sim. 2 – Control input of both methods.

Finally, the overall Guidance and Control system developed and presented in this work is implemented, revealing the main results of the UAV tracking to the vessel smoke plume. In this simulation a vessel moving in straight line is considered, with speed ratio of $\nu = 0.5$. As observed in Figure 8, the UAV starts in a random position behind the vessel and converges to the reference point using the control law with the proposed formulation. The smoke plume measurement sites are marked with a diamond, and are performed every $9.5s$ at a distance of 214 m from the vessel. In Figure 9 the distance between the vessel and the UAV is depicted, where it can be confirmed that the UAV never enters the keep-out area – with radius $r_{\text{min}} = 200$ m –, yet performing the smoke plume measurements relatively close to it.

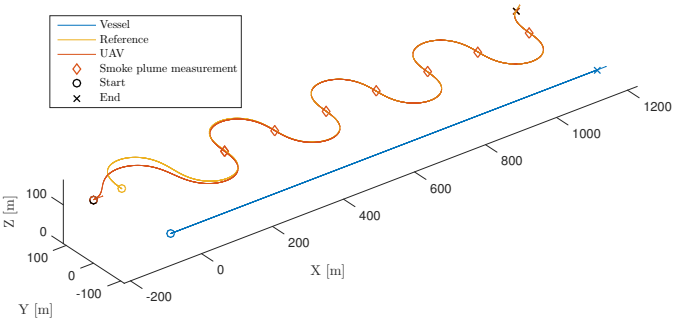

Figure 8: Sim. 3 – Trajectories of vessel, reference, and UAV

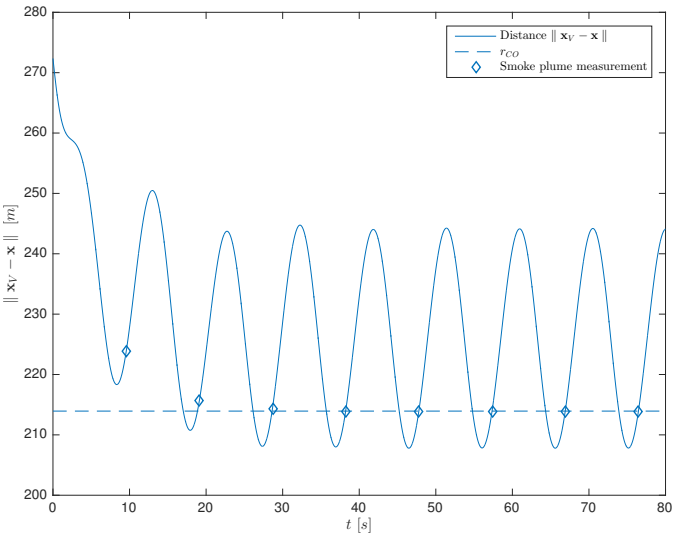

Figure 9: Sim. 3 – Distance between the vessel and the UAV

VI. Conclusion

Given the proposed mission of the UAV-based measurement of marine vessel smoke plumes, a Guidance and Control system was designed in order to command an autonomous fixed-wing UAV, providing enhanced conditions for the smoke measurements. The adopted path planning approach was considered to be a suitable solution to enable the consecutive crossings in a predefined point of the smoke plume, while dealing with the speed differential between both vehicles. During the controller design, a gap was found in the existing solutions in the literature, where this kind of tracking problem for nonholonomic vehicles with constant speed was not yet well-solutioned. A new formulation is proposed which eliminates the singularity in the posed tracking control problem, and global asymptotic stability of the controlled system was proved. Finally, the theoretical developments were supported with simulation results, and the overall system was implemented, achieving successfully all the proposed objectives.

References

[1] IMO, "Third IMO Greenhouse Gas Study 2014: Executive Summary and Final Report," Releasable to the Public.

[2] IMO, "MARPOL Annex VI, Sulphur oxides (SOx) - Regulation 14," Releasable to the Public.

[3] CompMon, "CompMon long term strategy," Releasable to the Public.

[4] W. Van Roy and K. Scheldeman, "Best Practices Airborne MARPOL Annex VI Monitoring," 2016.

[5] E. Lalish, K. A. Morgansen, and T. Tsukamaki, "Oscillatory Control for Constant-Speed Unicycle-Type Vehicles," in *Conference on Decision and Control*, pp. 5246–5251, IEEE, 2007.

[6] N. Regina and M. Zanzi, "UAV Guidance Law for Ground-based Target Trajectory Tracking and Loitering," in *Aerospace Conference*, pp. 1–9, IEEE, 2011.

[7] C. Samson and K. Ait-Abderrahim, "Feedback Control of a Nonholonomic Wheeled Cart in Cartesian Space," in *International Conference on Robotics and Automation*, pp. 1136–1141, IEEE, 1991.

[8] Y. Kanayama, Y. Kimura, F. Miyazaki, and T. Noguchi, "A Stable Tracking Control Method for a Non-Holonomic Mobile Robot," in *International Workshop on Intelligent Robots and Systems*, pp. 1236–1241, IEEE, 1991.

[9] R. Fierro and F. L. Lewis, "Control of a Nonholonomic Mobile Robot: Backstepping Kinematics Into Dynamics," in *Proceedings of the 34th IEEE Conference on Decision and Control*, vol. 4, pp. 3805–3810, IEEE, 1995.

[10] I. Kolmanovsky and N. H. McClamroch, "Developments in Nonholonomic Control Problems," *IEEE Control Systems*, vol. 15, no. 6, pp. 20–36, 1995.

[11] Z.-P. Jiang and H. Nijmeijer, "Tracking Control of Mobile Robots: a Case Study in Backstepping," *Automatica*, vol. 33, no. 7, pp. 1393–1399, 1997.

[12] A. A. J. Lefeber, *Tracking Control of Nonlinear Mechanical Systems*. Universiteit Twente, 2000.

[13] T.-C. Lee, K.-T. Song, C.-H. Lee, and C.-C. Teng, "Tracking Control of Unicycle-Modeled Mobile Robots Using a Saturation Feedback Controller," *IEEE Transactions on Control Systems Technology*, vol. 9, no. 2, pp. 305–318, 2001.

[14] K.-C. Cao, "Formation Control of Multiple Nonholonomic Mobile Robots Based on Cascade Design," in *Proceedings of the 48th IEEE Conference on Decision and Control*, pp. 8340–8344, IEEE, 2009.

[15] H. Khalil, *Nonlinear Systems, Upper Saddle River, New Jersey: Pretice-Hall Inc*. Pearson Education International, 2000.

[16] J.-J. E. Slotine, W. Li, *et al.*, *Applied Nonlinear Control*, vol. 199. Prentice hall Englewood Cliffs, NJ, 1991.

[17] P. Seibert and R. Suarez, "Global Stabilization of Nonlinear Cascade Systems," *Systems & Control Letters*, vol. 14, no. 4, pp. 347–352, 1990.

[18] V. Sundarapandian, "Global Asymptotic Stability of Nonlinear Cascade Systems," *Applied Mathematics Letters*, vol. 15, no. 3, pp. 275–277, 2002.

[19] V. Sundarapandian, "Local and Global Asymptotic Stability of Nonlinear Cascade Interconnected Systems," *Mathematical and Computer Modelling*, vol. 40, no. 1-2, pp. 227–232, 2004.

[20] E. Panteley and A. Lora, "On Global Uniform Asymptotic Stability of Nonlinear Time-Varying Systems in Cascade," *Systems & Control Letters*, vol. 33, no. 2, pp. 131–138, 1998.

[21] E. Panteley and A. Lora, "Growth Rate Conditions for Uniform Asymptotic Stability of Cascaded Time-Varying Systems," *Automatica*, vol. 37, no. 3, pp. 453–460, 2001.

[22] A. Lora and E. Panteley, "Cascaded Nonlinear Time-Varying Systems: Analysis and Design," *Advanced Topics in Control Systems Theory*, pp. 23–64, 2005.